Neutron Resonance Spectroscopy. XII. The Separated Isotopes of W†

H. S. Camarda,* H. I. Liou, G. Hacken, F. Rahn, W. Makofske, M. Slagowitz‡, S. Wynchank,§ and J. Rainwater
Columbia University, New York, New York 10533
(Received 14 May 1973)

The results of neutron resonance time-of-flight spectroscopy measurements using the Nevis synchrocyclotron are given for the separated W isotopes (182, 184, 186) and for natural W. Almost all s levels were observed to 2.65 keV, and resonance $(g)\Gamma_n^o$ values presented to ~16 keV for the above even isotopes, and to 700 eV and 2.6 keV, respectively, for ^{183}W. The ^{183}W level assignments were from levels in natural W which were not assigned to the other isotopes. A Bayes's theorem analysis shows that nearly all of the observed levels are s rather than p levels, since W is at a maximum for the s strength function S_0 but not for S_1, and the level detection sensitivity was not sufficient to detect other than exceptionally strong p levels. We were able to assign J values to 14 s levels of ^{183}W. The 41 observed ^{182}W levels to 2.65 keV and the 52 ^{183}W levels to 701 eV seem to be pure complete s populations, being fitted excellently by the Wigner nearest neighbor spacing theory and the Porter-Thomas reduced neutron width distribution. The orthogonal ensemble (OE) theory was found to be in good agreement with the ^{182}W and ^{183}W data. The ^{184}W level set to ~2.6 keV also seems to be an essentially complete, pure, s population sample. While it agreed within statistical limits to the above statistical theories, it gave poorer discrimination against alternate theories. Tests suggested that a few s levels in ^{186}W had been missed to ~2.6 keV. The $10^4 S_0$ values are 2.40 ± 0.31, 1.65 ± 0.32, 2.35 ± 0.24, and 2.23 ± 0.27 for 182, 183, 184, and 186, respectively. The $\langle D \rangle$ values for s populations are 66.3 ± 3.2 eV (182), 13.2 ± 0.7 eV (183), 81.3 ± 5.1 eV (184), and 90 ± 7 eV (186). A useful and accurate method for evaluating the Doppler-broadening integrals is described.

I. INTRODUCTION

This is the twelfth paper in a series[1-11] reporting neutron time-of-flight resonance spectroscopy measurements using the Columbia University Nevis synchrocyclotron. These measurements, using various thickness samples of the separated isotopes ^{182}W, ^{184}W, ^{186}W, and of natural W, were made during a major "run". The details of the experimental system during that run and of data analysis techniques were discussed in an earlier paper[8] reporting the results of similar studies for the separated Er isotopes.

A major reason for our interest in studying the even-A isotopes of W and many rare-earth nuclei ($150 \lesssim A \lesssim 190$) was to seek good test cases for theories predicting the statistical behavior of reduced neutron widths Γ_n^0, nearest neighbor level spacings D_J, and long- and short-range order or correlations. The published results for ^{166}Er provide the most convincing test case to date, giving confirmation of the statistical orthogonal ensemble (OE) theory for level spacing systematics as developed by Wigner, Dyson, Mehta, and others and discussed in Ref. 8. Supporting evidence was obtained from ^{168}Er, ^{152}Sm, ^{172}Yb, and other nuclei. A summary of the cases where we have found good confirmation of the OE theory predictions is given in *Statistical Properties of Nuclei*.[12] The case of ^{182}W, described in this paper, gives further strong support for the OE theory. The tungsten even-even isotopes have $I=0$ and form with s-wave neutrons compound-nuclear states characterized by the same spin and parity ($\frac{1}{2}^+$). These isotopes occur in the mass region of the split 4s peak in the s strength function S_0, where S_0 is appreciably stronger than the p strength function S_1. This enables one to measure, with an appropriate sample thickness, most or all of the s levels while including few if any p levels. Thus, the probability is high that a pure single population of s levels will be measured. Furthermore, these nuclei contain a statistically significant number of s levels over the energy region where the neutron time-of-flight facility has excellent resolution. The technique for this separation of weak p levels from s levels has been discussed in earlier papers.[8,13] The lowest mass even-A isotopes of reasonably high fractional abundance in the natural element seem, in each case, to give the best result because of their tendency to have greater level density, higher S_0 values, and lower S_1/S_0 values. The binding energy for an extra neutron is 6.19, 7.42, 5.75, and 5.46 MeV, respectively, for ^{182}W, ^{183}W, ^{184}W, and ^{186}W.

Neutron resonance spectroscopy studies of the tungsten isotopes also provide more detailed statistical information on the behavior of the s strength function vs the Z and A of the target nucleus. It is, for example, of interest to see if

"intermediate structure" variations in the intrinsic S_0 occur over relatively small energy regions compared with the energy scale for optical-model structure. Finally, tungsten is a refractory metal of interest for nuclear reactor design, so as thorough an understanding as possible of its interaction with neutrons is important for nuclear engineering purposes.

Following the series of measurements, all of the authors were involved in establishing the systematics needed to properly reduce the data to a transmission cross section (T, σ) vs E format for each sample measurement. The detailed analysis of the tungsten data was carried out by Camarda.[14] He has subsequently extended the analysis to include ^{183}W (using natural W). The results have been reviewed by the other authors. Extensive random matrix calculations carried out by Camarda have been discussed elsewhere[8,12] and will not be given here. Our detector sensitivities, counting times, and sample thicknesses were such that at most a few p levels are included in the reported level populations. While level parameters are given to ~13, 2.6, 16.5, and 17.4 keV, respectively, for isotopes 182, 183, 184, and 186, the missing of weak s levels becomes of significant and increasing importance above ~3 keV for the even-A isotopes. A significant portion of the ^{183}W levels in the natural W sample are rendered unobservable by the levels in the even isotopes.

While several experimental groups[15] have previously reported results for levels of the tungsten isotopes to a few hundred eV, the main other studies were made by Bartolome *et al.*[16] at the Rensselaer Polytechnic Institute (RPI) linac to a few keV for the even-A isotopes and to 760 eV for ^{183}W. Those measurements involved significantly poorer energy resolution than the results reported here but had higher level detection sensitivity, and consequently they include many very weak p-wave or spurious levels. For this reason, the present results give a much clearer picture of the s-wave systematics than do the RPI results.

II. EXPERIMENTAL CONDITIONS

The over-all aspects of synchrocyclotron operation during the run have been described.[8] The tungsten measurements mainly involved transmission measurements using our 200-m flight path, with supplementary measurements using our 40-m path. Self-indication measurements using the 40-m path provided some additional information, but the final results are based mainly on the transmission data. The eight thousand timing channels had $E_{\min} \approx 21$ eV for the 200-m data and ≈ 1 eV for the 40-m data. Natural tungsten has the following isotope A values and atomic abundances: (180–0.14%), (182–26.4%), (183–14.4%), (184–30.6%), and (186–28.4%). All have $I = 0$ except 183 which has $I = \frac{1}{2}$. About 100 g each of enriched ^{182}W, ^{184}W, and ^{186}W were obtained, having 94.4%, 94.3%, and 97.2% abundance, respectively, for the main isotope. These quantities of enriched oxides were divided into two or three different thickness samples of each isotope as summarized in Table I. The ^{180}W content is ignored here, but the positions of the known levels in ^{180}W below 100 eV (15.9, 49.3, 62.7, 75.2, and 87.4 eV) were checked to see that they were not attributed to ^{183}W in natural tungsten. They did not yield significant structure in the data.

III. DATA ANALYSIS AND RESULTS

The analysis for resonance parameters was similar to that described for Er.[8] The early stages of analysis yielded measured cross sections and transmissions for each sample vs energy. The σ vs E curves do not provide a good picture of the true behavior at resonances and the resonance cross-section behavior is best reconstructed from the tabulated Breit-Wigner level parameters in Tables II–V. The thick natural tungsten metal sample did, however, give reliable information on σ vs E between, but not too close to, levels. This information is plotted in Fig. 1. Many-channel averaging was used with the requirement that none of the averaged σ values deviate too far from the mean, or be too large. When two adjacent average sets satisfy these conditions, a line connects the points. The absence of a line between points implies that one or more resonances are present between them.

Published pre-1960 measured total cross-section results[17] for natural W below the first level at ~4 eV are reasonably self-consistent and are probably reliable. Above ~10 eV, where dense resonance structure is present, the previous lower resolution, measured total cross-section information for W tends to be misleading. In the regions of the resonances, the σ_t values are distorted by instrumental resolution and the choice of sample thicknesses. This is why the evaluation of resonance level parameters is best made via the measured T vs E rather than σ_t vs E curves, including the effects of instrumental resolution and of Doppler level broadening. As mentioned above, the best procedure for determining the true resonance σ vs E behavior is to use the Breit-Wigner formula and the evaluated resonance parameters. Interference terms between potential and resonance scattering can be evaluated using best choice scattering length (R') values for the resonance state

TABLE I. Separated and natural tungsten sample ($1/n$) values (b/atom) for the element and isotopes 182, 183, 184, and 186. The underlined values are for the principal isotope of the separated isotope samples.

Sample	Element	($1/n$) 182	183	184	186
^{182}W	120	<u>127.2</u>	4747	5176	15 000
^{182}W	461	<u>488</u>	18 200	19 800	57 500
^{182}W	920	<u>975</u>	38 500	42 000	121 900
^{184}W	95.9	5020	5130	<u>101.7</u>	5 020
^{184}W	432	24 000	24 500	<u>485</u>	24 000
^{184}W	865	48 000	49 000	<u>917</u>	48 000
^{186}W	122	33 000	40 500	6132	<u>125.7</u>
^{186}W	627	170 000	208 000	31 450	<u>645</u>
Nat W	11.92	44.7	82.4	38.9	42.5
Nat W	24.0	90.0	166	78.4	85.5
Nat W	47.7	179	330	156	170
Nat W	254	952	1760	830	904
Nat W	903	3380	6240	2950	3220

near resonance, due to the region average R' and the coherent resonance wing scattering contribution of nearby levels of the same (A, J, π). The σ_t vs E behavior between levels shown in Fig. 1 can provide checks for this process.

The between resonance measured σ_t vs E values for W, as shown in BNL-325, second edition[17] (p. 283) are misleadingly large. Similarly, there are problems in interpreting the measured σ_t vs E plot shown on p. 74-0-3 of the August 1966 supplement to BNL-325[18] in the energy region ~30 to 100 keV. In each case, the problem relates to the contribution of unresolved or partially resolved resonances to the measured values. Since the reasoning is somewhat complex, but important, a brief review of some of this logic is given below.

In a "poor resolution" measurement where all measured σ values tend to include some averaging over one or more resonances, the results tend to be very dependent on the sample thickness and the neutron energy. To suppress resonance contributions, a very thick sample should be used. For cases like the even W isotopes, where usually

TABLE II. Resonance parameters of ^{182}W. The asterisk indicates that the values for the 4.16-eV level are from Ref. 8.

E_0 (eV)	ΔE_0	Γ_n^0 (meV)	$\Delta\Gamma_n^0$	E_0 (eV)	ΔE_0	Γ_n^0 (meV)	$\Delta\Gamma_n^0$	E_0 (eV)	ΔE_0	Γ_n^0 (meV)	$\Delta\Gamma_n^0$	E_0 (eV)	ΔE_0	Γ_n^0 (meV)	$\Delta\Gamma_n^0$
* 4.16	0.02	0.72	0.02	2384.2	0.8	19	2	4961.2	2.4	5.4	0.7	8506	5	6.6	1.6
21.03	0.06	7.9	1.1	2411.9	0.8	4.3	0.6	5138.0	2.5	15.5	2.1	8533	5	6.6	1.6
114.39	0.13	23	3	2530.0	0.9	4.5	0.6	5199.1	2.6	72	6	8725	6	48	4
212.80	0.18	0.17	0.03	2575.9	0.9	17.7	2.0	5435.2	2.8	85	8	8815	6	20	3
248.01	0.22	57	4	2607.1	0.9	4.1	0.6	5538.2	2.9	7.7	2.0	9005	6	9.1	1.6
341.58	0.35	0.31	0.05	2790.2	1.0	54	5	5563.6	2.9	9.4	1.3	9231	6	42	4
376.16	0.40	7.4	1.0	2871.2	1.1	4.7	0.8	5655.7	3.0	186	27	9453	6	37	5
428.50	0.25	12.1	1.2	2940.9	1.1	5.4	0.7	5883.6	3.1	5.0	1.3	9473	6	12.8	3.6
484.16	0.30	20	2	3048.0	1.2	26	3	6018.8	3.2	3.1	1.3	9823	7	25	3
578.24	0.39	11.2	1.0	3118.9	1.2	3.0	0.5	6188.5	3.4	58	5	9896	7	16.5	2.0
655.22	0.46	5.2	0.8	3202.8	1.3	5.1	0.5	6259.1	3.4	33	4	9944	7	6.6	2.0
759.44	0.58	3.5	0.7	3256.9	1.3	10.5	0.9	6403.9	3.5	47	5	9998	7	32	6
781.70	0.60	0.33	0.09	3305.7	1.3	27	3	6514.1	3.6	11.3	1.9	10 025	7	33	6
862.76	0.34	0.78	0.14	3343.1	1.3	2.9	0.5	6535.7	3.6	23	3	10 140	7	16.5	2.0
918.78	0.38	11.4	1.3	3413.0	1.4	45	5	6605.1	3.7	4.7	1.0	10 260	7	37	4
947.26	0.40	65	7	3494.3	1.4	29	3	6667.9	3.8	59	6	10 603	8	18.2	2.4
1007.0	0.4	16.1	1.6	3522.8	1.5	8.6	1.0	6731.8	3.8	5.7	1.2	10 900	8	8.5	2.9
1095.1	0.5	44	6	3563.9	1.5	7.2	0.7	6743.1	3.8	7.7	1.2	11 000	8	17.5	1.9
1161.0	0.6	14.2	0.7	3602.1	1.5	21	3	6858.3	3.9	15.1	1.8	11 174	8	12.3	2.4
1274.9	0.6	1.09	0.17	3785.7	1.6	1.5	0.3	6960.5	4.0	34	4	11 310	8	30	3
1287.1	0.7	2.5	0.6	3846.2	1.7	74	9	7012.5	4.0	7.1	1.2	11 380	8	56	6
1325.9	0.7	0.69	0.22	3879.1	1.7	31	4	7101.8	4.1	5.8	1.2	11 560	8	24	3
1407.8	0.7	3.5	0.8	3975.1	1.7	27	3	7155.3	4.1	24	4	11 710	9	35	3
1502.0	0.8	11.4	0.8	3995.7	1.7	4.6	0.8	7243.1	4.2	12.7	1.8	11 780	9	5.9	1.4
1514.0	0.8	10.5	1.5	4062.3	1.8	17.9	2.8	7285.5	4.3	4.0	1.2	11 820	9	25	3
1582.0	0.9	1.96	0.38	4211.6	1.9	4.5	0.5	7472.1	4.4	45	4	11 890	9	29	3
1645.9	0.9	1.53	0.37	4266.4	1.9	3.2	0.5	7552.3	4.5	39	4	11 910	9	23	3
1772.0	.5	71	6	4312.5	2.0	30	3	7586.1	4.5	6.2	1.2	12 210	9	17.6	2.7
1793.1	0.5	5.9	1.0	4367.4	2.0	1.3	0.3	7693.6	4.7	44	4	12 361	9	9.9	2.7
1920.9	2.0			4431.3	2.0	44	4	7744.6	4.8	14	2	12 490	10	29	3
2006.1	0.6	32	3	4492.5	2.0	6.6	0.8	7810.4	4.8	34	3	12 540	10	26	3
2061.0	0.7	29	3	4714.8	2.2	13.8	1.5	7834.1	4.8	14.7	2.8	12 680	10	18	3
2103.9	0.7	6.9	0.6	4832.2	2.3	43	5	8012.7	4.9	14.8	2.2	13 057	10	27	3
2179.9	0.7	12.7	1.1	4846.0	2.3	2.2	0.5	8192.4	5.1	18.1	2.2	13 180	10	44	6
2225.9	0.7	17	2	4911.3	2.4	19.4	2.9	8394.0	5.3	19.9	2.7	13 253	10	29	3
2328.2	0.8	11.7	1.2												

TABLE III. Resonance parameters for ^{183}W. Those levels having "a" before the energy were identified as ^{183}W levels by the RPI group and are considered by us to be ^{183}W levels.

E_0 (eV)	ΔE_0	$g\Gamma_n^0$ (meV)	$\Delta g\Gamma_n^0$	E_0 (eV)	ΔE_0	$g\Gamma_n^0$ (meV)	$\Delta g\Gamma_n^0$	E_0 (eV)	ΔE_0	$g\Gamma_n^0$ (meV)	$\Delta g\Gamma_n^0$	E_0 (eV)	ΔE_0	$g\Gamma_n^0$ (meV)	$\Delta g\Gamma_n^0$
7.63	0.03	0.40	0.11	347.27	0.18	5.3	0.5	690.1	0.5	0.84	0.19	1625.9	0.9	2.1	0.2
27.05	0.03	6	1	a352.83	0.18	0.027	0.016	695.1	0.5	5.7	1.1	1662.9	0.9	2.0	0.7
40.68	0.03	0.20	0.05	360.39	0.19	1.3	0.2	700.6	0.5	0.59	0.13	1685.0	0.5	0.56	0.17
46.24	0.07	14.1	2.2	377.56	0.20	3.6	1.6	752.0	0.6	4.4	0.7	1710.1	0.5	4.8	1.5
47.85	0.04	3.8	0.4	390.86	0.21	1.1	0.2	807.8	0.6	0.70	0.18	1738.0	0.5	1.6	0.4
65.34	0.03	0.18	0.03	417.78	0.23	1.2	0.3	852.1	0.3	0.34	0.10	1754.0	0.5	1.1	0.4
101.10	0.12	6.5	1.0	425.36	0.24	0.73	0.24	862.6	0.4	1.36	0.34	1819.9	0.5	2.6	0.6
103.90	0.12	0.19	0.03	430.70	0.25	1.93	0.72	867.3	0.4	0.51	0.30	1836.0	0.5	5.1	0.8
138.00	0.09	0.18	0.03	459.75	0.27	0.40	0.07	869.4	0.4	3.1	1.4	1856.9	0.6	6.2	0.7
144.22	0.10	2.0	0.2	a468.23	0.56	0.092	0.023	893.9	0.4	1.5	0.3	1866.0	0.6	3.5	1.2
154.40	0.11	8.7	1.2	a492.74	0.30	0.045	0.022	940.9	0.4	1.3	0.3	1870.1	0.6	3.9	1.4
157.01	0.11	3.2	0.6	a495.14	0.30	0.036	0.018	1059.1	0.5	0.40	0.15	1955.1	0.6	1.9	0.5
173.82	0.25	3.0	0.5	a512.48	0.32	0.053	0.022	1062.9	0.5	1.14	0.31	1992.9	0.6	3.9	0.8
192.09	0.15	2.1	0.4	534.61	0.34	0.54	0.15	1114.0	0.5	0.63	0.15	2144.2	0.7	4.3	0.9
a203.19	0.16	0.06	0.02	550.71	0.35	1.96	0.34	1141.0	0.5	10.1	1.2	2158.2	0.7	4.7	0.9
a229.15	0.40	0.03	0.02	558.22	0.36	2.1	0.4	1151.0	0.5	0.80	0.24	2167.1	0.7	4.9	0.9
235.06	0.20	0.27	0.04	567.73	0.37	0.76	0.21	1176.0	0.6	0.79	0.12	2219.1	0.7	7.6	1.5
240.28	0.20	0.46	0.09	571.07	0.37	1.51	0.29	1241.0	0.6	7.5	1.0	2237.1	0.7	2.1	1.0
258.89	0.20	3.2	0.4	587.88	0.39	0.83	0.12	1313.1	0.7	3.2	0.6	2260.1	0.7	1.2	0.5
279.61	0.25	6.0	0.6	603.00	0.41	1.96	0.41	1369.9	0.7	3.5	0.8	2280.9	0.8	2.5	0.6
a288.13	0.26	0.018	0.012	608.30	0.41	0.45	0.16	1451.1	0.8	0.68	0.13	2315.9	0.8	6.9	1.5
296.33	0.14	0.99	0.11	646.58	0.45	4.8	0.6	1541.0	0.8	1.0	0.2	2443.8	0.8	13	2
321.82	0.16	3.2	0.5	675.91	0.48	1.58	0.31	1567.0	0.9	0.76	0.15	2640.2	0.9	4.3	0.8
336.96	0.17	0.21	0.03												

TABLE IV. Resonance parameters of ^{184}W.

E_0 (eV)	ΔE_0	Γ_n^0 (meV)	$\Delta\Gamma_n^0$	E_0 (eV)	ΔE_0	Γ_n^0 (meV)	$\Delta\Gamma_n^0$	E_0 (eV)	ΔE_0	Γ_n^0 (meV)	$\Delta\Gamma_n^0$	E_0 (eV)	ΔE_0	Γ_n^0 (meV)	$\Delta\Gamma_n^0$
101.69	0.11	0.36	0.05	2982.2	1.1	15	2	6965	4	11.6	1.8	11450	8	8.4	2.3
168.90	0.13	0.03	0.03	3133.2	1.2	8	1	7049	4	74	8	11650	9	10.6	1.9
184.17	0.14	81	7	3181.8	1.2	18	3	7122	4	18.6	3.6	11710	9	64	6
242.85	0.21	0.13	0.03	3202.8	1.2	39	4	7205	4	5.1	1.2	11819	9	50	6
310.66	0.30	4.3	0.3	3232.2	1.3	5.8	0.5	7303	4	22	3	11850	9	84	9
422.85	0.24	2.1	0.2	3457.1	1.4	39	4	7335	4	9.8	1.8	12020	9	10.2	3.2
681.23	0.49	25	2	3539.3	1.4	22	3	7472	4	76	7	12170	9	12.2	2.3
703.68	0.51	0.24	0.04	3596.2	1.5	1.4	0.4	7552	5	71	7	12432	9	21	2
784.09	0.60	0.57	0.11	3735.9	1.6	53	4	7777	5	13.5	2.8	12658	10	13.7	2.2
799.34	0.62	62	5	3807.3	1.6	67	7	8167	5	40	4	13001	10	37	4
957.32	0.40	45	5	3941.0	1.7	4.5	0.8	8310	5	16.6	2.7	13082	10	8.4	2.0
998.55	0.43	2.6	0.3	4007.9	1.7	6.2	1.6	8458	5	58	7	13201	10	174	22
1086.0	0.5	94	9	4186.5	1.9	40	4	8549	5	55	5	13361	5	29	4
1132.0	0.5	10.1	1.5	4249.3	1.9	16.3	2.3	8603	6	12.3	2.2	13390	5	32	4
1261.0	0.6	37	3	4546.6	2.1	8.8	1.5	8741	6	11.7	2.1	13480	5	60	8
1334.9	0.7	0.42	0.11	4614.5	2.1	4.9	0.9	8889	6	19.9	2.1	13499	5	3.6	1.4
1399.9	0.7	86	5	4802.4	2.3	27	3	8987	6	12.7	2.6	13610	5	6.7	1.7
1423.9	0.7	20	2	4927.9	2.4	24	4	9046	6	81	7	13681	5	15	2
1514.0	0.8	37	4	5053.4	2.5	6.7	1.0	9286	6	22	3	13831	6	31	4
1551.8	0.8	2.2	1.0	5090.4	2.5	39	4	9372	6	66	6	14419	6	92	13
1655.0	0.9	6.4	0.7	5188.8	2.6	22	3	9665	7	6.1	1.5	14861	6	50	6
1792.1	0.5	29	4	5807.1	3.0	5.9	1.0	9816	7	14.7	3.5	15071	6	11	2
1920.1	0.6	5.5	0.7	5883.6	3.1	67	9	9843	7	33	4	15170	6	16	2
2045.1	0.6	27	2	6067.0	3.2	5.1	0.8	10050	7	50	5	15250	6	18	2
2092.1	0.7	99	10	6127.3	3.3	146	32	10249	7	102	9	15351	7	15	2
2210.9	0.7	5.9	0.6	6232.1	3.4	12.2	2.5	10418	7	10.9	2.5	15449	7	74	12
2252.0	0.7	10.5	0.8	6411.0	3.5	2.8	1.0	10682	8	33	4	15631	7	150	20
2411.1	0.8	27	3	6474.7	3.6	9.3	1.2	10739	8	8.9	2.4	15971	7	87	16
2459.2	0.8	12	1	6548.4	3.6	8.4	1.2	11070	8	86	9	16201	7	29	3
2540.0	0.9	13	2	6788.8	3.8	12	2	11280	8	30	4	16318	7	31	4
2620.8	0.9	25	2	6913.0	3.9	4.5	1.2	11371	8	9.1	2.4	16451	7	15	3
2836.2	2.0														
2921.9	1.1	39	4												

$\Gamma_n > \Gamma_\gamma$ for s levels and only a single s population is involved, the destructive interference between potential and resonance scattering may, in extreme cases, give a measured σ_t less than σ_{pot}. For intermediate thickness samples, one obtains $\sigma_{meas} = \sigma_{pot}$ plus a contribution of a fraction of $\langle\sigma_{res}\rangle$, this fraction decreasing rapidly with increasing sample thickness. For a very thin sample, $\langle\sigma_{res}\rangle$ averaged over several levels has the following form for s levels:

$$\langle\sigma_{res}\rangle = (410)(1\text{ eV}/E)^{1/2}(10^4 S_0)\text{ b/atom}.$$

Since $10^4 S_0 \approx 2$ for W, this gives $\sim 800(1\text{ eV}/E)^{1/2}$ b/atom.

If σ_{meas} is to be a true representation of $\langle\sigma_t\rangle$, a very thin sample must be used such that $n\sigma$ is always $\ll 1$, even at resonance. When $\Gamma_n \gg \Gamma_\gamma$ as is approximately true for the even W isotopes, such a thin single isotope sample must have $(1/n) > 2.6 \times 10^6 (1\text{ eV}/E)$ b/atom, which implies $n\langle\sigma_{res}\rangle$ is less than $\sim 3 \times 10^{-4}(E/1\text{ eV})^{1/2}$. This value is so small that the average sample transmission is too close to unity to achieve good accuracy for a determination of $\langle\sigma_t\rangle$ except well above 10-keV neutron energy. When a mixture of isotopes is involved, as for natural W, the condition is correspondingly relaxed.

The analysis for the resonance level parameters was similar to that performed for Er[8] and other cases.[9-11] For each plot of measured neutron transmission vs energy, and for each sample thickness, the "area" of the transmission dip yields an implied functional relation between Γ and Γ_n (or $g\Gamma_n$). The implied curves of Γ_n vs Γ for each measurement and sample thickness tend to have different average slopes (sample-thickness-dependent) near their points of intersection. Such plots were made for each resonance to determine Γ_n (and possibly Γ_γ). Since the curves are similar to the examples shown in Refs. 8–11, we have not included any examples in this paper. The intersection point should be consistent with $\Gamma \approx \Gamma_n + \langle\Gamma_\gamma\rangle$ since Γ_γ values for different levels do not vary greatly from $\langle\Gamma_\gamma\rangle \approx 65$ meV for the tungsten levels. In most cases, this latter condition on Γ was used to help establish the Γ_n values. The analysis included the effects of Doppler broadening (room temperature) and the interference between potential and resonance scattering. An effective $R' = 7.0$ fm was used. The levels (even A) tended to have $\Gamma_n > \Gamma_\gamma$ which made determination of a precise Γ_γ difficult. The intersection of the various curves was generally consistent with $\Gamma \approx \Gamma_n + \langle\Gamma_\gamma\rangle$. For levels in the upper part of the energy range, one curve for the

TABLE V. Resonance parameters of ^{186}W.

E_0 (eV)	ΔE_0	Γ_n^0 (meV)	$\Delta\Gamma_n^0$	E_0 (eV)	ΔE_0	Γ_n^0 (meV)	$\Delta\Gamma_n^0$	E_0 (eV)	ΔE_0	Γ_n^0 (meV)	$\Delta\Gamma_n^0$	E_0 (eV)	ΔE_0	Γ_n^0 (meV)	$\Delta\Gamma_n^0$
18.80	**0.06**	**74**	**7**	2875.9	1.1	18.7	1.9	6489.0	3.6	63	5	10 271	7	21	3
170.72	**0.12**	**2.1**	**0.3**	2976.1	1.1	2.1	0.6	6697.9	3.8	3.0	0.7	10 349	7	82	9
217.46	**0.18**	**32**	**3**	3038.8	1.1	202	22	6754.5	3.8	49.9	4.3	10 580	7	10.3	2.4
286.66	**0.27**	**1.9**	**0.4**	3158.0	1.2	43	4	6948.6	4.0	13.2	1.8	10 629	7	29	4
405.66	**0.45**	**4.5**	**0.4**	3312.3	1.3	13.6	1.6	6968.5	4.0	21	2	10 769	8	34	4
509.63	**0.32**	**4.1**	**0.4**	3423.3	1.4	60	5	7114.1	4.1	6.9	1.1	10 850	8	106	14
541.28	**0.35**	**21**	**2**	3540.7	1.4	8.4	1.0	7176.1	4.2	16.5	1.8	11 749	9	33	4
663.10	**0.47**	**24**	**1**	3713.4	1.5	2.7	0.8	7324.0	4.3	8.0	1.2	11 868	9	10.5	3.7
719.80	**0.53**	**76**	**6**	3768.2	1.6	25	2	7472.1	4.4	64	6	12 309	9	72	14
831.05	**0.33**	**1.1**	**0.1**	3870.8	1.7	52	5	7633.9	4.6	19.9	2.3	12 408	9	100	18
963.02	**0.41**	**33**	**3**	3963.1	1.7	11.1	1.1	7712.1	4.6	26.9	2.9	12 590	10	37	9
1071.0	0.5	15.7	1.8	4165.2	1.8	24	2	7843.6	4.8	11.3	2.3	12 619	10	71	15
1121.1	0.5	11.5	1.2	4221.0	1.9	42	4	7978.4	4.9	11.8	1.7	13 201	10	27	4
1187.1	0.6	25	2	4395.1	2.0	29	3	8131.8	5.0	8.7	1.1	13 320	8	17.8	4.3
1418.0	0.7	2.3	0.3	4540.3	2.1	33	3	8294.9	5.2	29	3	13 569	5	51	8
1500.0	0.8	33	3	4804.7	2.3	87	4	8436.9	5.2	9.6	2.2	14 021	6	30	5
1794.9	0.5	0.6	0.2	4975.6	2.4	6.4	1.7	8625.1	5.5	9.4	1.9	15 199	6	66	10
1933.1	0.6	17.7	1.8	5158.3	2.5	38	3	8669.1	5.5	6.9	1.7	15 439	7	49	12
2025.0	0.6	12.6	1.4	5282.2	2.6	5.7	0.8	9176.6	6.0	43	4	15 478	7	47	12
2104.9	0.7	3.8	0.8	5383.5	2.7	14.5	2.0	9200.8	6.0	2.8	1.0	15 651	7	152	24
2349.1	0.8	5.0	0.6	5402.5	2.7	7.4	0.8	9285.9	6.1	88	9	15 718	7	22	5
2514.8	0.9	15.0	1.5	5667.3	2.9	70	5	9409.7	6.3	94	9	16 491	7	68	12
2589.8	0.9	20	2	5777.0	3.0	68	5	9542.3	6.4	31	6	16 630	7	75	12
2658.9	0.9	94	6	6293.1	3.4	17.0	1.9	9587.1	6.4	279	31	16 931	8	61	9
2779.2	1.0	8.2	1.3	6386.4	3.5	22	3	9842.7	6.7	24	3	17 060	8	11	5
												17 299	8	45	8
												17 342	8	9.5	3.0

thickest sample was supplemented by the $\Gamma = \Gamma_n + \langle \Gamma_\gamma \rangle$ curve to establish Γ_n. At lower energies the presence of a given isotope as a small impurity in another isotope provides an additional helpful (very thin sample) analysis curve. The natural W samples were useful for the even isotopes. They provided the entire basis for the ^{183}W analysis after excluding the even-A levels. However, a significant portion of the energy interval was unavailable for ^{183}W level analysis due to masking by strong even-A isotope levels.

Our set of ^{183}W levels consists of those which are observed in the natural W sample, but are not identified as belonging to the even isotopes. As can be seen from Table I, the isotopic thickness for each isotope in the thickest natural sample is significantly greater than that for any of the separated isotope samples. Although most even isotope levels have $g\Gamma_n$ values large enough to be seen in the separated even-isotope samples, there are also some levels in the natural W which would not have been seen in the even-A isotope samples even if they had been even-A isotope levels. Within this class of resonances, those levels, in Table III, having "a" before the energy were identified as ^{183}W levels by the RPI group[16] and are considered by us to be ^{183}W levels. Many of the weaker levels reported by the RPI group for ^{183}W were not seen in our data and are not included in our list.

The ^{183}W level analysis in certain cases gave a significantly superior fit using either $J=0$ or $J=1$ rather than the opposite choice. We favor $J=0$ for the levels at 47.85, 154.4, 258.9*, 695.1, and 1710 eV, and $J=1$ for the levels at 27.05, 46.24, 101.1*, 279.6, 321.8, 347.3, 646.6, 1241, and 1313 eV. The levels with asterisks above have the opposite J favored in the BNL-325 listings[17] which extend to ~420 eV, or by the RPI results[16] to 760 eV.

Some weak levels which were observed but not identified as belonging to any particular W isotope have not been included in the main tables. These unidentified levels might be ^{180}W resonances. The following listing gives each resonance energy followed by the corresponding $ag\Gamma_n$ value (in meV) in parentheses: (74.85 ± 0.03) eV (0.04 ± 0.02), (107.6 ± 0.1) eV (0.025 ± 0.01), (356.5 ± 0.2) eV (0.12 ± 0.06), (373.9 ± 0.2) eV (0.21 ± 0.10), and (613.7 ± 0.4) eV (0.22 ± 0.10).

The thickest ($1/n = 125.7$ b/atom) ^{186}W sample shows a very wide asymmetrical transmission dip structure for the 18.8-eV level, mainly due to the interference between potential and resonance scattering (Fig. 2). In this case, there is a large fractional change in E over the range, so the energy dependence of Γ_n must be included in the Breit-Wigner resonance formula. An excellent shape fit from 9 to 25 eV was obtained using $\Gamma_n = 310$ meV (at 18.8 eV), and $R' = 7.5$ fm. The use of a constant R' for all levels is not really justified since it includes the effect of neighboring levels of the same isotope. However, the analysis is not very dependent on the choice of R' for most levels when $1/n \gtrsim 100$ b/atom for the sample, as is true for these separated isotope samples.

The data analysis for the resonance parameters requires that the effect of Doppler broadening of the cross section near resonance be included. In the Appendix, we give a brief account (taken from

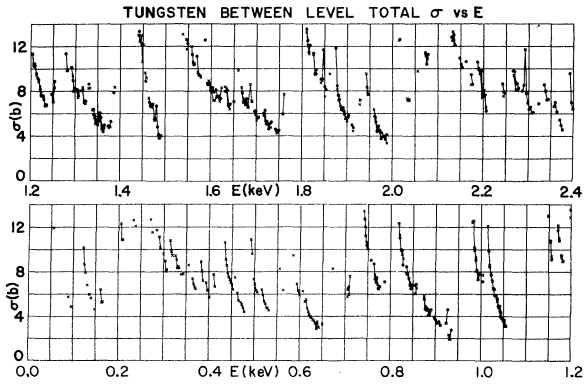

FIG. 1. The between level total cross section vs energy for natural tungsten to 2.4 keV. The × and ⊙ denote the local measured average cross section obtained with sample thickness $1/n = 11.9$ for different but overlapping energy regions. The plotted points satisfy the requirements that none of the individual cross sections within an averaging group exceed a certain value or deviate significantly from the group mean (or else the average is not plotted). If two adjacent average cross sections are used, they are connected by a line.

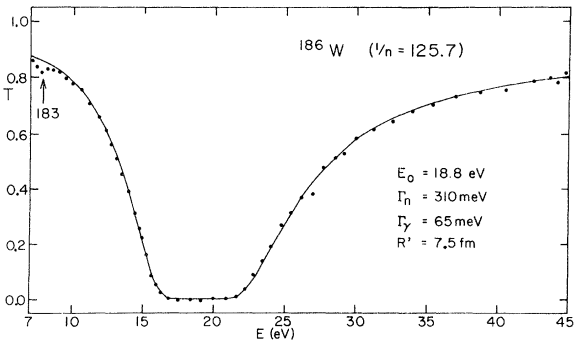

FIG. 2. Result of a shape fit to the measured transmission of the ^{186}W separated isotope with $1/n = 125.7$ b/atom for the 18.8-eV level, using a Breit-Wigner single level formula with the parameters indicated in the figure. The analysis includes Doppler broadening and the $(E)^{1/2}$ variation of Γ_n. The arrow shown in the figure indicates the position of a ^{183}W isotope impurity level.

Ref. 14) of an accurate and efficient method for evaluating the Doppler-broadening integrals. This method has been used for all of our level analysis over the past few years where "partial shape" analysis is used, or where "wing corrections" are involved in level transmission dip "area analysis".

IV. THE SYSTEMATICS OF THE RESULTS

Figures 3(a)–3(d) show the cumulative number of observed resonances N vs neutron energy E for ^{182}W, ^{183}W, ^{184}W, and ^{186}W, respectively. The figures all show an initial energy region of nearly linear slope which extends to about 4.4 keV for ^{182}W, 701 eV for ^{183}W, 4.2 keV for ^{184}W, and 5.7 keV for ^{186}W, and decreasing slope at higher energies. Since a Bayes's theorem analysis indicates that the vast majority of our reported levels are unlikely to be p levels, the main problem at higher energies is from missed weak s levels. The above energy limits are the upper energies above which a significant number of s levels are being missed. The figures include various visually fitted straight lines which imply mean s-level spacings $\langle D\rangle$, but not our final choices. The detailed procedure of our final choices for $\langle D\rangle$ will be described at the end of the paper.

Figures 4(a)–4(d) give plots of $\sum\Gamma_n^0$ or $\sum g\Gamma_n^0$ for

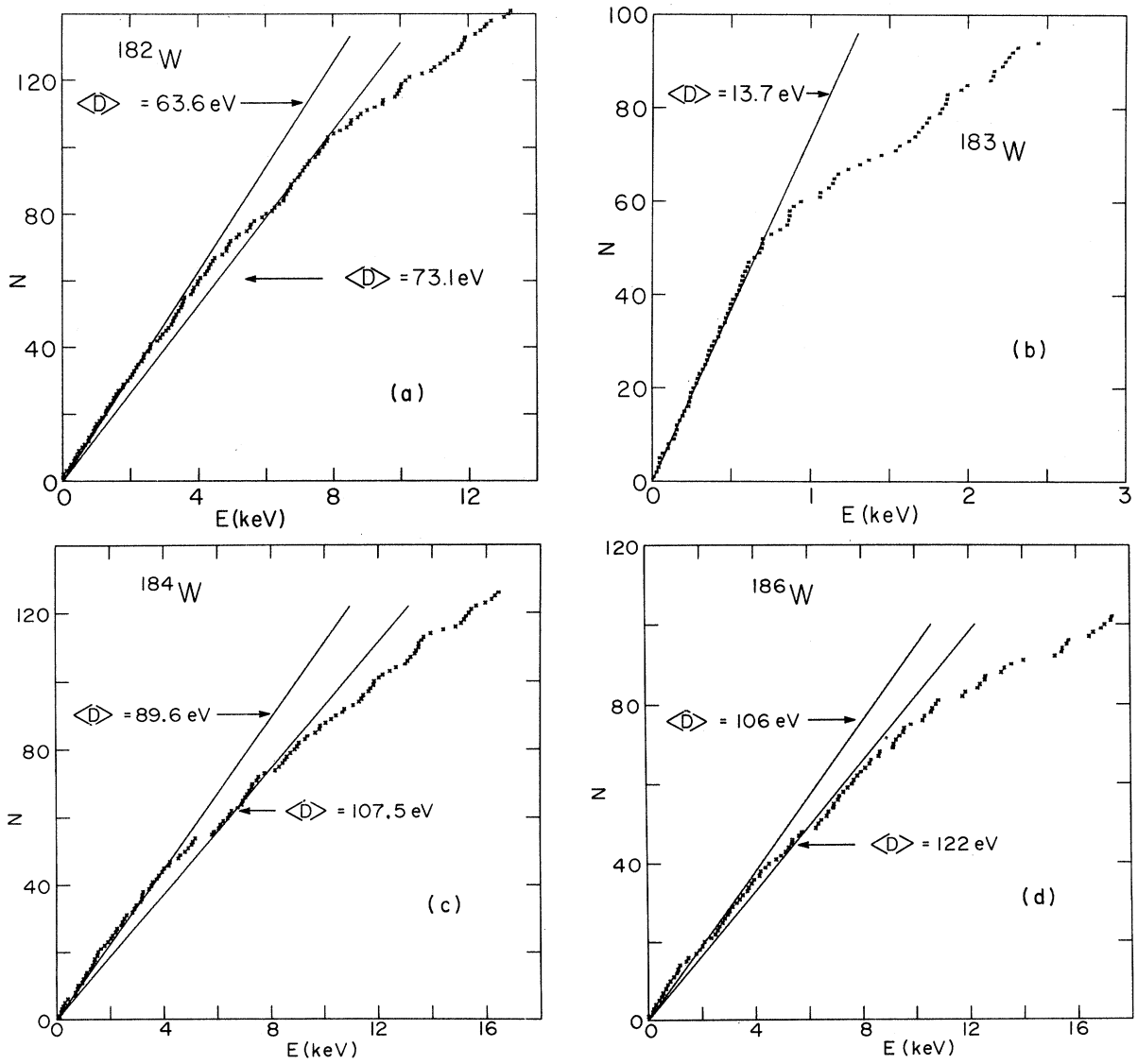

FIG. 3. Plots of the cumulative number of observed levels vs energy for (a) ^{182}W, (b) ^{183}W, (c) ^{184}W, and (d) ^{186}W. The values of $\langle D\rangle$ shown in the plots represent the slopes of various visually fitted straight lines. The final choices of $\langle D\rangle$ for the tungsten isotopes are discussed in the text and are given in Table VII.

the four isotopes. The slopes of the plots correspond to the s strength functions. Since missed weak levels have negligible effect on these plots, it is valid to use larger energy intervals for the S_0 evaluations, unless one believes that increasing systematic errors in the Γ_n^0 values occur at the higher energies where the energy resolution is much poorer. The plots for the even-A isotopes are consistent with a single S_0 over their ranges when one considers the size of the fluctuations expected for a randomly drawn single-channel Porter-Thomas (PT) sample from a distribution having a common $\langle\Gamma_n^0\rangle$. The experimental values for ^{183}W are in poorer agreement with a common slope and undoubtedly are influenced by missed levels where the even-A isotope levels in natural W mask the ^{183}W levels.

An attempt to compare our results with those of the RPI group shows that there is rough agreement for Γ_n^0 values for most resonances in the even-A isotopes, but the agreement is poorer for ^{183}W where they list Γ_n and Γ_n^0 without always specifying how Γ_n^0 was obtained (assumed J value). There are also a number of inconsistencies in their values indicating evaluation or typographical errors. A few examples are as follows: There is a mutual inconsistency between their Γ_n and Γ_n^0 values for their ^{183}W levels at 258 and 750 eV. Their $g\Gamma_n^0$ values above about 500 eV are systematically much larger than ours and are quite incompatible with our results in many cases. Their Γ_n^0 values for ^{182}W are in reasonable general agreement for most levels, but we suspect that their quoted values are 10 times too large for their levels at 1273, 1285,

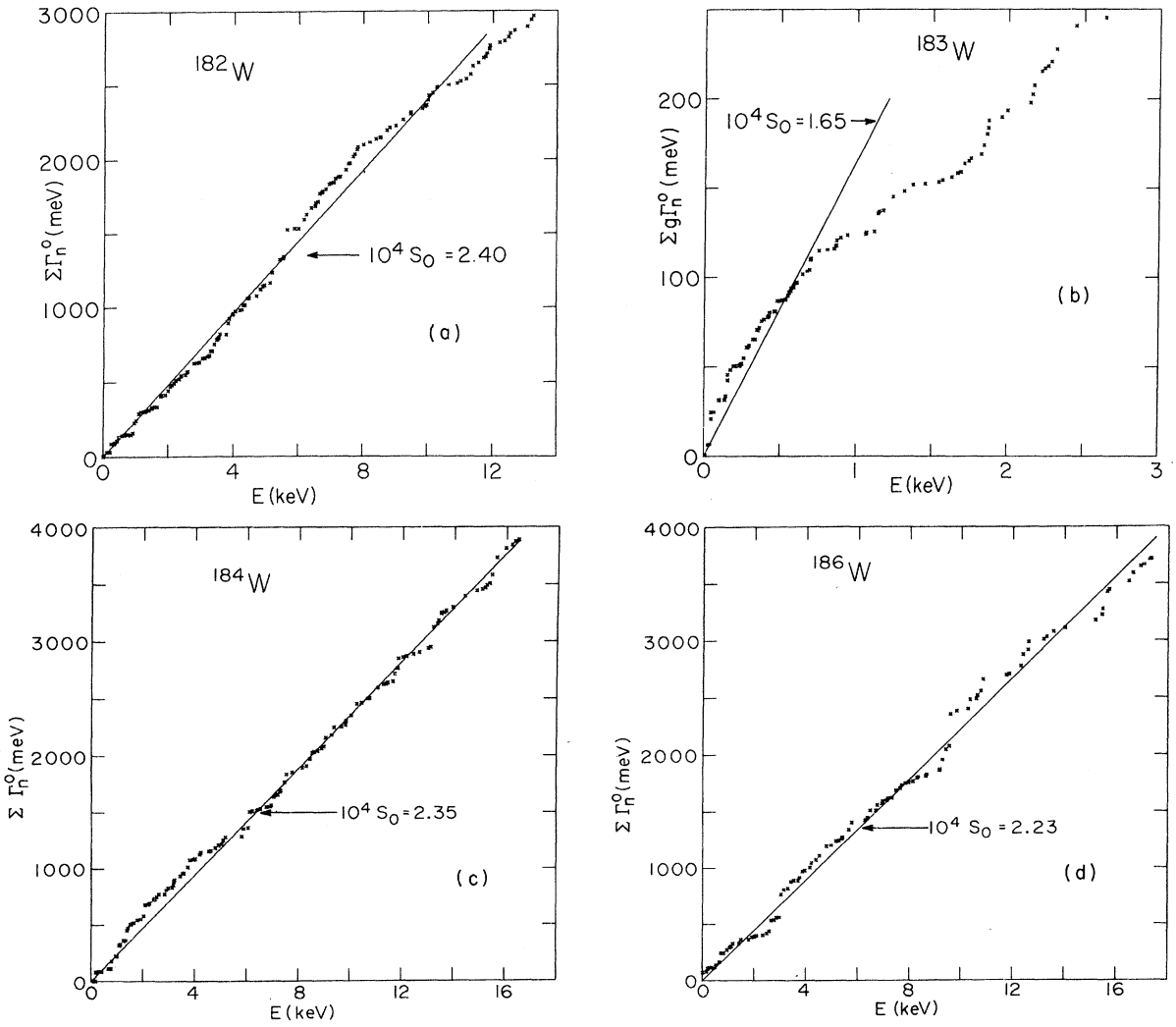

FIG. 4. Plots of $\sum\Gamma_n^0$ (or $g\Gamma_n^0$) vs energy for (a) ^{182}W, (b) ^{183}W, (c) ^{184}W, and (d) ^{186}W. The slopes of the straight lines give the s strength functions, S_0. For ^{183}W a number of strong levels are missed above 800 eV since they are masked by even-isotope levels in natural sample data.

1324, 1578, 1644, 1790, and 2100 eV. These large, probably incorrect Γ_n^0 values increase their strength functions above our results.

The distribution of $(\Gamma_n^0)^{1/2}$ values for 182, 184, 186, and $(g\Gamma_n^0)^{1/2}$ for 183 are compared with the (PT) theory in Figs. 5(a)–5(d) where equal $\langle g\Gamma_n^0\rangle$ values are used for the two spin states in 183. The plots for the even isotopes exhibit two energy regions, the region below 2650 eV, and also a larger energy region of 7.8 keV for 182, and 10 keV for 184 and 186. The agreement with the PT theory is fairly good for the lower energy regions where most levels are included, but a gross missing of weaker levels is indicated above these energies. The comparison of the experimental histograms and the PT theory for the larger energy intervals is made on the basis of $\langle D\rangle$ values (see Table VII) obtained from the lower energy regions. This procedure should give valid fits except for the smaller $(\Gamma_n^0)^{1/2}$ portion of the plots (missed

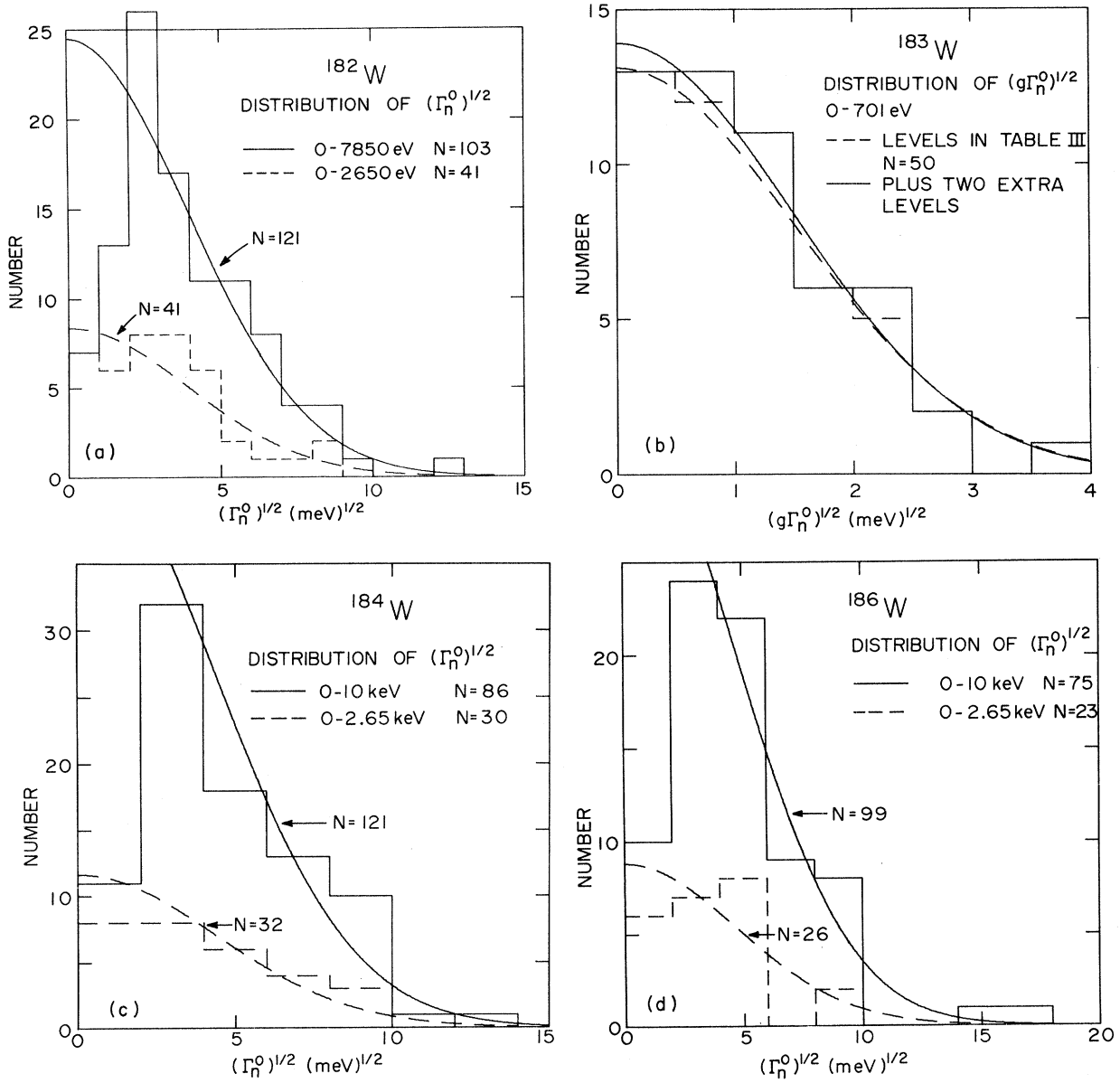

FIG. 5. Histograms of $(\Gamma_n^0)^{1/2}$ or $(g\Gamma_n^0)^{1/2}$ values for (a) ^{182}W, (b) ^{183}W, (c) ^{184}W, and (d) ^{186}W. For the even isotopes, histograms are shown for two energy intervals. The experimental results are compared with Porter-Thomas distributions which are normalized to the experimental S_0 value, with the total number of levels in each energy interval calculated from the best choices for $\langle D\rangle$. For ^{183}W, histograms and theoretical curves are shown for (i) the levels in Table III and (ii) adding two extra levels at 244.5 and 479 eV (as discussed in text).

weak levels). This is seen to be the case. Figure 5(b) for ^{183}W displays both the situations where just resonances to 701 eV in Table III are included, and where extra levels at 244.5 and 479 eV are added. These two levels could not be observed in our natural tungsten data because they are masked by resonances of other isotopes. The 244.5-eV level is weak but was observed by RPI[16] and others.[17] The 479-eV level is strong and easily identified as belonging to ^{183}W. The fits for 183 with the PT theory are fairly good in both cases.

Figures 6(a)–6(d) exhibit the experimentally observed nearest neighbor level spacing distributions for 182, 183, 184, and 186 and the distributions predicted by the Wigner theory. The comparisons are made only over the energy regions where essentially all *s* levels are included. For 183 the experimental and predicted spacing distributions are given to 701 eV, with and without the extra levels at 244.5 and 479 eV. Both fits are seen to

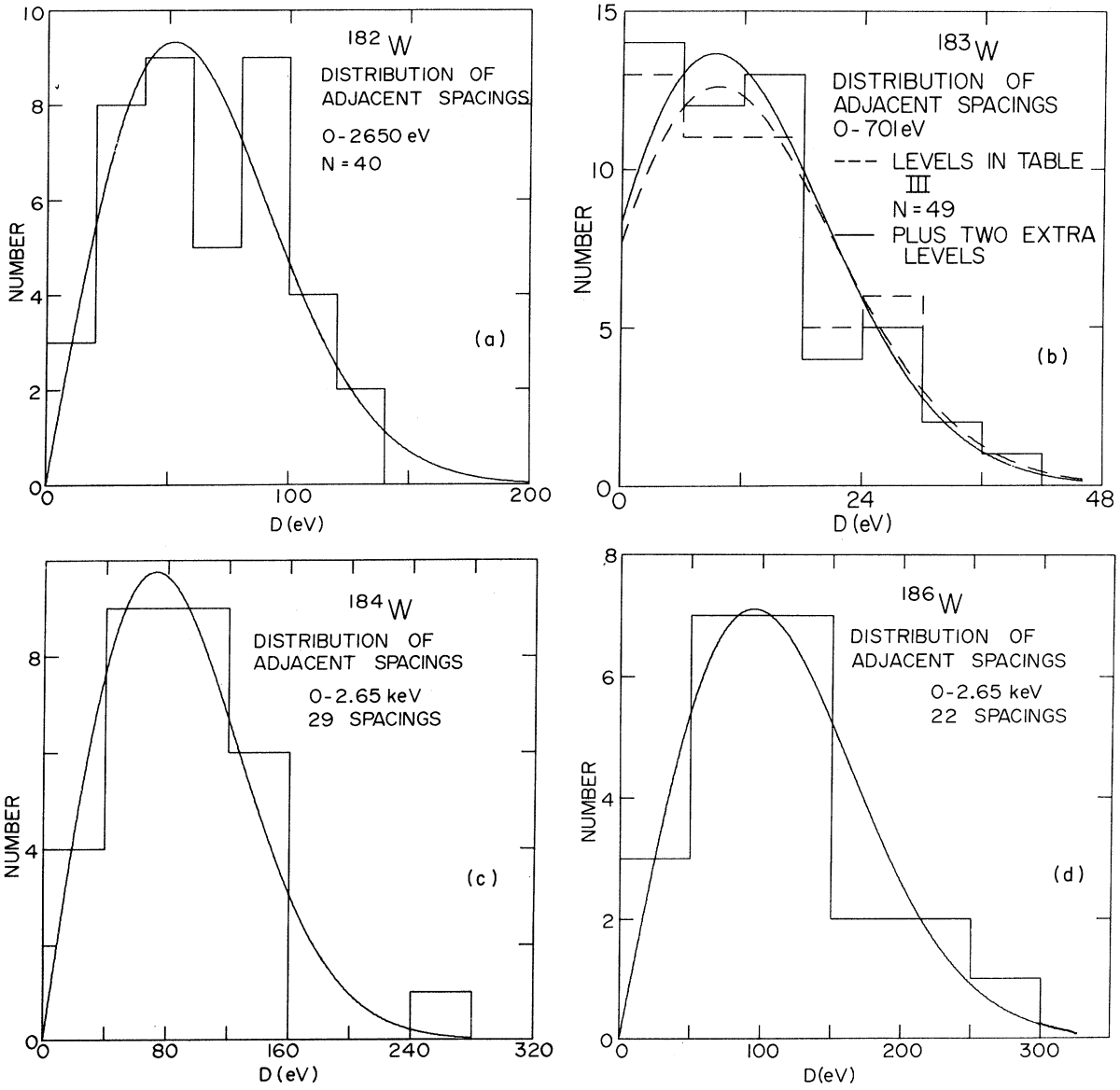

FIG. 6. Plots of the nearest neighbor level spacing histograms and the Wigner distributions (normalized using the total number of levels N in each energy interval calculated from the proper choice of $\langle D \rangle$) for (a) ^{182}W, (b) ^{183}W, (c) ^{184}W, and (d) ^{186}W. For ^{183}W, the theoretical curves are for a merged two-population distribution with the relative density in the ratio of $(2J+1)$ values. The curves, and histograms for ^{183}W are given for (i) the levels in Table III and (ii) adding two extra levels (see text).

be fairly good.

Figures 7(a)–7(d) show the best-fit straight lines to the N vs E staircase plots for 182, 183, 184, and 186. For reasons given below, the ^{184}W resonance at 168.9 eV is not included in the plot. The goodness of fit is given by the Dyson-Mehta Δ statistic of the OE theory, which is the mean square deviation of the staircase $N(E)$ from the best-fit straight line. These results are summarized in Table VI. We also list in Table VI the experimental values for the correlation coefficients $\rho(S_i, S_{i+1})$, for nearest neighbor level spacings, and the values of the combined statistic $(\Delta+\rho)$, as in Refs. 8–11. The OE theory predicts a standard deviation of 0.11 for Δ_{D-M} (see Table VI) for the single population even-A cases, and 0.22 for ^{183}W where two merged populations are involved. The theoretical predictions for $\rho(S_i, S_{i+1})$ are $-0.273 \pm 0.92N^{-1/2}$ for a single population (even-A isotopes) and -0.21 ± 0.09 for two merged populations (183) with $N=90$, and where $J=0$ and $J=1$ states comprise $\frac{1}{4}$ and $\frac{3}{4}$ of the total level population, respectively. The theoretical values are based mainly on our Monte Carlo studies of the type discussed in Ref. 8. For the uncorrelated Wigner (UW) case each nearest neighbor level spacing is assumed to be randomly generated according to the Wigner distribution, with a common population $\langle D \rangle$, with

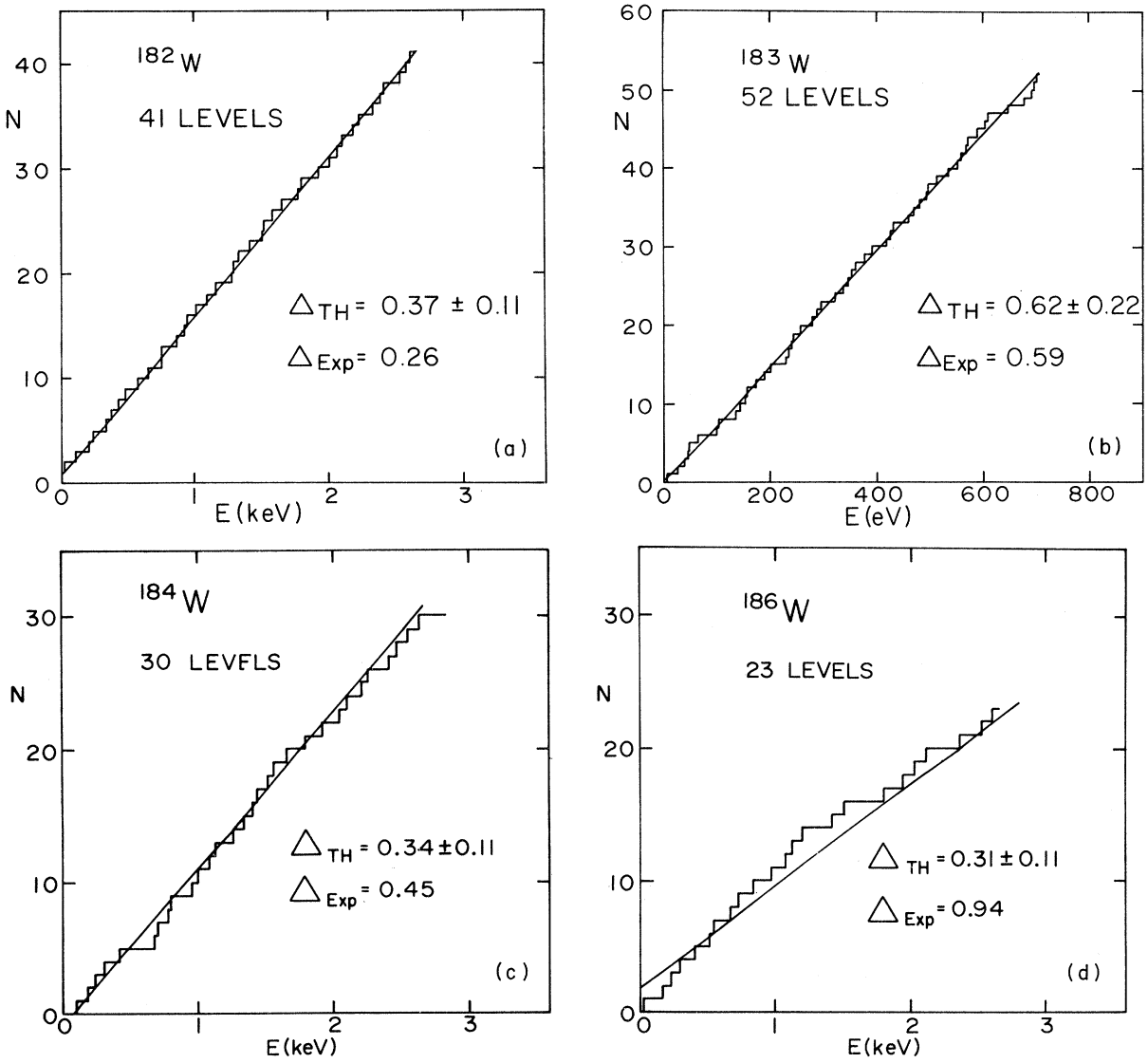

FIG. 7. Plots of the best straight line fits to N vs E for (a) ^{182}W, (b) ^{183}W, (c) ^{184}W, and (d) ^{186}W with the experimental and theoretical values obtained from the Dyson-Mehta Δ test. For ^{183}W, levels are included to 701 eV. For the even isotopes, levels are included to 2650 eV.

TABLE VI. Summary of the results of statistical OE tests Δ and $\rho(S_i, S_{i+1})$, for the tungsten isotopes. The labels are as follows: A: all levels in Table III; B: plus extra levels at 244.5 and 479 eV seen by RPI but not by us; C: all levels in Table IV; D: excluding the weak level at 168.9 eV.

Isotope	Level selection	E_{max} (keV)	n	Δ_{D-M}	Δ_{exp}	$\rho(S_i, S_{i+1})$	$(\Delta+\rho)$	$P_<$(OE)	$P_<$(UW)
182	all	2.65	41	0.369	0.259	−0.369	−0.110	0.10	0.0025
183	A	0.701	50	0.609	0.484	−0.158	0.326		
183	B	0.701	52	0.617	0.594	−0.091	0.503		
184	C	2.65	31	0.341	0.469	−0.228	0.241	0.74	0.20
184	D	2.65	30	0.338	0.446	−0.284	0.162	0.71	0.16
186	all	2.65	23	0.311	0.939	−0.075	0.864	1.00	0.86
186	all	1.23	14	0.260	0.168	−0.295	−0.127	0.22	0.036

no long- or short-range correlations.

An examination of Table VI indicates the predictions of the OE theory are in good agreement with the 41 levels of ^{182}W which we believe to be a pure single population of s-wave resonances. The agreement is also good for ^{183}W to 701 eV with or without the levels at 244.5 and 479 eV.

The ^{184}W data show an improbably large, 259.6 eV, nearest neighbor spacing between the levels at 422.85 and 681.23 eV [see Fig. 6(c)]. This increases the experimental Δ value. This energy region is one where we have excellent ability to detect other than extremely weak levels. The absence of an observed level may reflect a true large statistical fluctuation in the spacing distribution, or a missed very weak s level. In any event, the effect is to make the ^{184}W data poor for distinguishing between the OE and UW theories. This is partly related to the difficulty of making such distinctions when relatively small level populations are involved. The strong distinction for ^{182}W relates to the fact that the experimental Δ and ρ values both differ by about 1 standard deviation from the OE predictions in the direction of giving a less positive $(\Delta+\rho)$ value, while the opposite tends to be true for ^{184}W. The statistical tests performed on ^{186}W suggest that a significant number of s levels were missed above ~1200 eV, below which there are only 14 levels. This makes comparison with theories of low statistical significance even though there is good agreement with OE theory below 1200 eV.

A Bayes's theorem analysis of all the even-A tungsten levels for $E<2650$ eV indicates that only the 168.9-eV level of ^{184}W has a significant probability (0.8) for being p wave, assuming the $l=1$ strength function to be 1.0×10^{-4}. Cases C and D in Table VI display results of statistical tests obtained using data sets including and excluding this resonance. The difference between cases C and D is not statistically significant.

Figure 8 shows the result of the Bohigas-Flores $\sigma(k)$ test[19] for ^{182}W and for ^{184}W data to 2.65 keV excluding the 168.9-eV level. In this test, one examines the spacing distribution for levels having k levels between them. Here $\sigma(k)$ is the standard deviation of the spacing distribution from its mean in units of $\langle D\rangle$, for each choice of k. This test is sensitive to short-range order extending over a few level spacings in addition to that for just the nearest neighbor spacings. While both ^{182}W and ^{184}W have $\sigma(k)$ values mainly within the 10 and 90% confidence limits expected for the OE theory, the ^{182}W values are on the low side while the ^{184}W values are on the high side. This feature, as for ρ and Δ, has ^{182}W strongly favor the OE case over the UW or two-body random matrix ensemble (TBRE) cases, while the distinction is less clear for ^{184}W. A detailed discussion of these theories can be found in Ref. 8.

The Dyson F-statistic test[13] is designed to de-

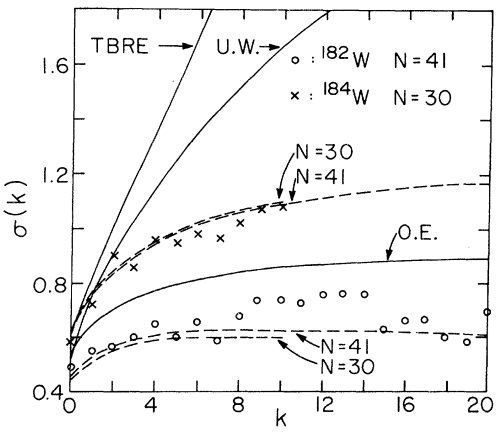

FIG. 8. Comparison of experimental results for ^{182}W and ^{184}W to 2650 eV for $\sigma(k)$ vs k with Monte Carlo results for OE, UW, and TBRE theories. $\sigma(k)$ is the standard deviation from the mean for the spacings of levels having k levels in between (in units of $\langle D\rangle$). The dashed curves give the 10 and 90% confidence limits for OE for the two isotopes.

TABLE VII. Final choices of $l=0$ average nearest neighbor spacings and s-wave strength functions for the tungsten isotopes.

Isotope	$\langle D\rangle$ (eV)	$10^4 S_0$
182	66.3 ± 3.2	2.40 ± 0.31
183	13.2 ± 0.7	1.65 ± 0.32
184	81.3 ± 5.1	2.35 ± 0.24
186	90 ± 7	2.23 ± 0.27

tect the presence of spurious levels or missing levels in an otherwise perfect single population of levels. Calculations of F vs energy for ^{182}W to 2.6 keV, similar to those given in Ref. 11 for ^{172}Yb, indicate that the OE predictions are in excellent agreement with the ^{182}W data.

A summary of our best choices for $\langle D\rangle$ and the s strength functions S_0 is given in Table VII. The values of $\langle D\rangle$ for ^{182}W and ^{183}W are derived from the slopes of the straight line fits to $N(E)$ [Figs. 7(a) and 7(b)]. The results of this evaluation are essentially indistinguishable from those obtained using an optimum statistic for $\langle D\rangle$, as was done in Ref. 8 for erbium data (which had a larger number of levels in its complete populations). For ^{184,186}W, the final choices of $\langle D\rangle$ were made by estimating the probable number of s levels missed in each case. The uncertainties in $\langle D\rangle$ and S_0 quoted in Table VII are based on considerations discussed in Ref. 11.

ACKNOWLEDGMENTS

We wish to thank Dr. George Rogosa of the U.S. Atomic Energy Commission for providing help in procuring the separated isotope samples. The computer interface system was developed by the Pegram Laboratory electronics group under Dr. Jack Hahn, with contributions from Dr. Hugo Ceulemans. Technical support by the late Arthur Blake, Lester Morganstein, and William Van Wart was important.

APPENDIX: EVALUATION OF THE DOPPLER-BROADENING INTEGRALS

The Doppler-broadening integrals have the form:

$$\psi(B,x)=\frac{1}{B\sqrt{\pi}}\int_{-\infty}^{+\infty}\frac{e^{-(x-y)^2/B^2}}{1+y^2}\,dy,$$

$$\chi(B,x)=\frac{1}{B\sqrt{\pi}}\int_{-\infty}^{+\infty}\frac{ye^{-(x-y)^2/B^2}}{1+y^2}\,dy.$$

On pages 302 and 303 of the *Handbook of Mathematical Functions*[20] are listed two integrals of particular interest. They are:

$$\int_{-\infty}^{+\infty}\frac{y'e^{-t^2}dt}{y'^2+(x'-t)^2}=\pi\mathrm{Re}W(x'+iy'),$$

$$\int_{-\infty}^{+\infty}\frac{(x'-t)e^{-t^2}dt}{y'^2+(x'-t)^2}=\pi\mathrm{Im}W(x'+iy').$$

x' is real, $y'>0$, where $W(Z)$ is defined as

$$W(Z)=e^{-Z^2}[1-\mathrm{erf}(-iZ)].$$

These integrals bear a striking resemblance to the Doppler-broadening integrals. With an elementary change of variables, it can be shown that

$$\psi(B,x)=\frac{\sqrt{\pi}}{B}\mathrm{Re}W\left(\frac{x}{B}+i\frac{1}{B}\right),$$

$$\chi(B,x)=\frac{\sqrt{\pi}}{B}\mathrm{Im}W\left(\frac{x}{B}+i\frac{1}{B}\right).$$

The only remaining problem is how to calculate the complex error function rapidly and accurately. Instructions for doing this are given in the handbook mentioned above.

---

†Research supported in part by the U.S. Atomic Energy Commission.

*Present address: National Bureau of Standards, Gaithersburg, Maryland.

‡Present address: New Jersey Department of Higher Education, Trenton, New Jersey.

§Present address: University of Capetown, Republic of South Africa.

[1]J. L. Rosen, J. S. Desjardins, J. Rainwater, and W. W. Havens, Jr., Phys. Rev. 118, 687 (1960), ^{238}U.

[2]J. S. Desjardins, J. L. Rosen, W. W. Havens, Jr., and J. Rainwater, Phys. Rev. 120, 2214 (1960), Ag, Au, Ta.

[3]J. B. Garg *et al.*, Phys. Rev. 134, B985 (1964), ^{232}Th, ^{238}U.

[4]J. B. Garg, J. Rainwater, J. S. Peterson, and W. W. Havens, Jr., Phys. Rev. 136, B177 (1964), As, Br.

[5]J. B. Garg, J. Rainwater, and W. W. Havens, Jr., Phys. Rev. 137, B547, (1965), Nb, Ag, I, Cs.

[6]S. Wynchank, J. B. Garg, W. W. Havens, Jr., and J. Rainwater, Phys. Rev. 166, 1234 (1968), Mo, Sb, Te, Pr.

[7]J. B. Garg, J. Rainwater, and W. W. Havens, Jr., Phys. Rev. C 3, 2247 (1971), Ti, Fe, Ni.

[8]H. I. Liou *et al.*, Phys. Rev. C 5, 974 (1972), Er.

[9]F. Rahn *et al.*, Phys. Rev. C 6, 251 (1972), Sm, Eu.

[10]F. Rahn et al., Phys. Rev. C 6, 1854 (1972), ^{232}Th, ^{238}U.

[11]H. I. Liou *et al.*, Phys. Rev. C 7, 823 (1973), Yb.

[12]H. S. Camarda *et al.*, in *Statistical Properties of Nuclei*, edited by J. B. Garg (Plenum, New York, 1972), pp. 205–213.

[13]H. I. Liou, H. S. Camarda, and F. Rahn, Phys. Rev. C 5, 1002 (1972).
[14]H. S. Camarda, Ph. D. thesis, Columbia University, 1970 (unpublished).
[15]F. A. Khan and J. A. Harvey, Nucl. Sci. Eng. 25, 31 (1966); R. C. Block, R. W. Hockenbury, and J. E. Russel, ORNL Report No. ORNL-3924, 1965 (unpublished), p. 31; ORNL Report No. ORNL-3778, 1964 (unpublished), p. 53; F. W. K. Firk and M. C. Moxon, Nucl. Phys. 12, 552 (1959); C. Corge *et al.*, C. R. Acad. Sci. (Paris) 249, 413 (1959); R. B. Schwartz, V. E. Pilcher, and R. M. Schechtman, Bull. Am. Phys. Soc. 1, 187 (1956).
[16]Z. M. Bartolome, R. W. Hockenbury, W. R. Moyer, J. R. Tatarzuk, and R. C. Block, Nucl. Sci. Eng. 37, 137 (1969).
[17]*Neutron Cross Sections,* compiled by D. J. Hughes and R. B. Schwartz, Brookhaven National Laboratory Report No. BNL-325 (U.S. GPO, Washington, D.C., 1958), 2nd ed.; *Neutron Cross Sections,* compiled by D. J. Hughes, B. A. Magurno, and M. K. Brussel, Brookhaven National Laboratory Report No. BNL-325 (U.S. GPO, Washington, D.C., 1960), 2nd ed., 1st suppl.
[18]*Neutron Cross Sections,* compiled by M. D. Goldberg, S. F. Mughabghab, S. N. Purohit, B. A. Magurno, and V. M. May, Brookhaven National Laboratory Report No. BNL-325 (U.S. GPO, Washington, D.C., 1966), 2nd ed., 2nd Suppl., Vol. IIC, $Z = 61-87$.
[19]O. Bohigas and J. Flores, in *Statistical Properties of Nuclei,* edited by J. B. Garg (Plenum, New York, 1972), pp. 195–203.
[20]*Handbook of Mathematical Functions with Formulas, Graphs and Mathematical Tables,* edited by M. Abramowitz and I. Stegun (Dover, New York, 1964), pp. 302–303.